Preprints.org

Article

Not peer-reviewed version

Hydrogen Sulfide (H_2S) Adsorption from Natural Gas Using Silver Modified 13X Molecular Sieve

Mirzokhid Abdirakhimov , Mohsen H. Al-Rashed , Janusz Wójcik *

Posted Date: 5 December 2023

doi: 10.20944/preprints202312.0233.v1

Keywords: H₂S adsorption; 13X molecular sieve; adsorption capacity; ion exchange; silver modification

Preprints.org is a free multidiscipline platform providing preprint service that is dedicated to making early versions of research outputs permanently available and citable. Preprints posted at Preprints.org appear in Web of Science, Crossref, Google Scholar, Scilit, Europe PMC.

Copyright: This is an open access article distributed under the Creative Commons Attribution License which permits unrestricted use, distribution, and reproduction in any medium, provided the original work is properly cited.

Preprints (www.preprints.org) | NOT PEER-REVIEWED | Posted: 5 December 2023 doi:10.20944/preprints202312.0233.v1

Disclaimer/Publisher's Note: The statements, opinions, and data contained in all publications are solely those of the individual author(s) and contributor(s) and not of MDPI and/or the editor(s). MDPI and/or the editor(s) disclaim responsibility for any injury to people or property resulting from any ideas, methods, instructions, or products referred to in the content.

Article

Hydrogen Sulfide (H_2S) Adsorption from Natural Gas Using Silver Modified 13X Molecular Sieve

Mirzokhid Abdirakhimov [1], Mohsen H. Al-Rashed [2] and Janusz Wójcik [1,*]

Abstract: The removal of H_2S from natural gas and other gases such as biogas, refinery gases, and coal gas is required because H_2S is toxic and corrosive, even in traces. Zeolites are widely used in the removal of H_2S from the above-mentioned gases. In this work, we prepared an Ag-exchanged 13X molecular sieve by using different concentrations of $AgNO_3$ to increase its adsorption properties. XRD, SEM, and BET techniques were used to characterize samples. When compared to unmodified 13X, the adsorption capacity of AgII-13X increased by about 50 times. The results of this study suggest that the silver-modified 13X molecular sieve is highly effective at extracting H_2S from natural gas.

Keywords: H_2S adsorption; 13X molecular sieve; adsorption capacity; ion exchange; silver modification

1. Introduction

When compared to other fuels, natural gas produces fewer greenhouse gases during combustion. According to the International Energy Agency (IEA) [1], it covers over one-third of global energy consumption and is expected to expand substantially in all scenarios. Although natural gas is considered a pure fuel, it contains carbon dioxide (CO_2), hydrogen sulfide (H_2S), and other sulfur compounds such as mercaptans (R-SH), carbonyl sulfide (COS), and carbon disulfide (CS_2) that need to be removed. The term "sour natural gas" refers to natural gas that contains hydrogen sulfide [2]. Because H_2S is toxic and corrosive in nature, even a trace amount of it should be removed or reduced substantially. To meet the natural gas sales specification, the H_2S concentration must be less than 4 ppmv [3]. The procedure of sweetening of natural gas entails the extraction of acid gases, with a primary focus on hydrogen sulfide (H_2S). There exist four distinct methodologies employed for the removal of H_2S, including absorption, adsorption, membrane separation, and cryogenic distillation. Absorption and adsorption are widely recognized processes employed in the natural gas sector for the removal of acid gases. This methodology primarily relies on the selective absorption of H_2S and CO_2 gases using various solvents. Alkanolamine solvents and their blends are extensively utilized as solvent [4,5]. The process of absorption involves a chemical reaction between acid gases and solvents; hence, it is referred to as chemisorption. The process is characterized by high energy consumption, as well as issues related to equipment corrosion and solvent loss. Adsorption is the process by which molecules adhere to the adsorbent's surface. In this process, activated carbon [6–8] , MOFs [9,10], metal oxides [11,12] and zeolites [13,14] are commonly used to eliminate H_2S from various gases. The adsorbents that were described before each have their own set of drawbacks, which prevents them from being utilized in industrial settings. In the case of activated carbon, for instance, it possesses a high adsorption capacity and is superior to other adsorbents; yet its regeneration process is very challenging. Metal oxides exhibit a high affinity for H_2S, but they have a poor surface area and a lack of pores [15]. Furthermore, they are able to demonstrate their activity at high temperatures, which leads to increased costs related to energy consumption and obstacles in the process. However, zeolites are preferable to other adsorbents for their characteristics, such as high temperature stability, large surface area, regenerability, and low cost. They are crystalline aluminosilicates of alkaline and alkaline earth metals. Their open 3-dimensional framework structures are made of corner-sharing AlO_4 and SiO_4 tetrahedra. Adsorbents such as Linde Type A

© 2023 by the author(s). Distributed under a Creative Commons CC BY license.

Preprints (www.preprints.org) | NOT PEER-REVIEWED | Posted: 5 December 2023 doi:10.20944/preprints202312.0233.v1

(4A, 5A) and Faujasite (13X) molecular sieves are widely used in industry to remove acid gases. The use of 13X Faujasite zeolite for the extraction of H_2S from different combination mixtures has shown promising results [16–19].

As a result of the increased demand for natural gas usage, the sour components contained in it will have to be reduced appreciably. This requires the synthesis of new adsorbents or improvements in the adsorption properties of the existing ones. The introduction of various metals, such as Cu, Zn, Co, and Ag, into zeolites has been extensively studied to increase the adsorption performance toward H_2S. Barelli et. al. [20] conducted a study on the use of Cu exchanged 13X for the removal of H_2S from biogas and found that it exhibits high adsorption capacity in a wide range of operating conditions. Chen et.al. [21] studied the adsorption performance of AgX, CoX and ZnX zeolite synthesized by ion-exchanging of X zeolite for Claus tail gas desulfurization. The authors reported that AgX has a high adsorption capacity for H_2S and COS in comparison to other samples. Kumar et.al. [22] investigated Ag and Cu modified X and Y Faujasite to remove H_2S from gas streams containing He, N_2, CO_2, CO, and H_2O. The experiments were carried out at both room temperature and 150°C. AgX and AgY were capable to adsorb H_2S as despite the presence of other gases while CuX and CuY failed in the presence of 2% CO. It was found that Ag exchanged Faujasite has strong selectivity towards H_2S whereas Cu exchanged Faujasite is susceptible to CO adsorption. Kulawong et al. [23] examined Ag exchanged NaX zeolite as a means of removing H_2S from an anaerobic digestor reactor. The author's findings revealed that an increase in the loading of Ag positively impacts the adsorption of H_2S. As mentioned earlier, H_2S is mainly found with methane in various gases including biogas, natural gas, refinery gas, coal gas and other gases. Therefore, in order to assess adsorbents in a real-world setting, it is crucial to conduct tests using real gas mixtures. The aforementioned research attempts utilized a diverse range of synthetic gases instead of natural gas. To our knowledge, there has been an absence of study pertaining to the adsorption of H_2S from methane.

In this work, we conducted experiments with a real natural gas mixture to study the effect of Ag-modified 13X molecular sieves on the removal of H_2S. Ag-modified 13X samples were prepared by ion-exchange method. In addition, we investigated the effect of the inlet H_2S concentrations and exchange rates of the Ag ions on the adsorption operation. The current study shown significant efficacy in the development of a silver exchanged 13X molecular sieve utilized for the extraction of H_2S from natural gas.

2. Materials and Methods

2.1. Reagents and materials

The substrate materials were conventionally available 13X molecular sieve (from Hurtland LLC, Poland), $AgNO_3$ (from Stanlab LLC, Poland), Methane 2.5 (Siad Poland LLC, Poland), 5000 ppm H_2S in CH_4 (from Air Liquide Polska LLC) and deionized water.

2.2. Synthesis of Ag ion exchanged 13X

Ag ion exchanged 13X was prepared by stirring 10 g of 13X molecular sieve in various molar concentrations of $AgNO_3$ water solution (0.02M, 0.05M, and 0.1M in 200 ml) for 24 h. Ag ion exchanged 13X molecular sieves were labelled as AgI-13X, AgII-13X, and AgIII-13X, respectively. Then the samples were washed with deionized water, filtered, and dried at 110°C for 12 h. Calcination was done at 600°C for overnight in the oven. Samples were cooled and kept in a desiccator.

2.3. Characterization

The phase composition of samples was determined using a powder X-ray diffractometer (Seifert 3003TT) with a Cu X-ray tube ($k\lambda1$ =1.540598Å, $k\lambda2$ =1.544426Å, $k\beta$ =1,39225Å). The powder samples were analyzed between 5° and 80° of 2Theta with 0.05° step. In order to validate the crystal structures, the X-ray diffraction patterns that were acquired were compared with the information that was collected from the Joint Committee on Powder Diffraction Standards (JCPDS). Morphological features of the sample surface were obtained by Scanning Electron Microscope (SEM) images using

Preprints (www.preprints.org) | NOT PEER-REVIEWED | Posted: 5 December 2023 doi:10.20944/preprints202312.0233.v1

a Phenom ProX SEM (Phenom-World BV, Eindhoven, The Netherlands). The elemental analysis of the samples were also carried out by energy dispersive X-ray spectroscopy (EDS) during SEM image acquisition. The BET surface of the samples was measured using a Micromeritics ASAP 2020 adsorption analyzer, Micromeritics Inc., Norcross, GA, USA.

2.4. H_2S gas separation

A laboratory scale set-up was used to carry out H_2S adsorption, as shown in Figure 1. 10 g of adsorbent was placed in the Teflon adsorber (40 mm long and 1.5 mm internal diameter) and attached to the system. The primary objective of employing 10 g of adsorbent is to replicate the authentic process, as the flow rate of 400 mL/min may prevent H_2S molecules present in methane coming into contact with the surface of the adsorbent. As a result, analyzers in the outlet flow may quickly detect the presence of H_2S gas that is not in direct contact with the adsorbent, allowing for the early detection of breakthrough time. The installation was carefully checked to ensure all connections had no leakage. The mixture was fed directly to a scrubber unit until the desired H_2S concentration in methane was achieved. Mixtures composed of various concentrations of H_2S were introduced at the top of the adsorption column with a flow rate of 400 mL/min under atmospheric pressure. The flow rate of the mixed gas was controlled by the rotameter to maintain a flow rate of 400 mL/min. To measure initial and breakthrough H_2S concentrations, two analyzers (Southland Sensing Ltd., USA) were installed prior to and after the adsorber. Analyzers are able to measure the concentration of hydrogen sulfide in a broad range, from 0 to 2000 ppm. H_2S concentrations were recorded in the input and output every second to obtain accurate results. Outlet gas was treated with a NaOH solution and burned before being released. Phenolphthalein was used to indicate the H_2S saturation of the NaOH solution. Pipelines and fittings made of stainless steel were used to prevent corrosion.

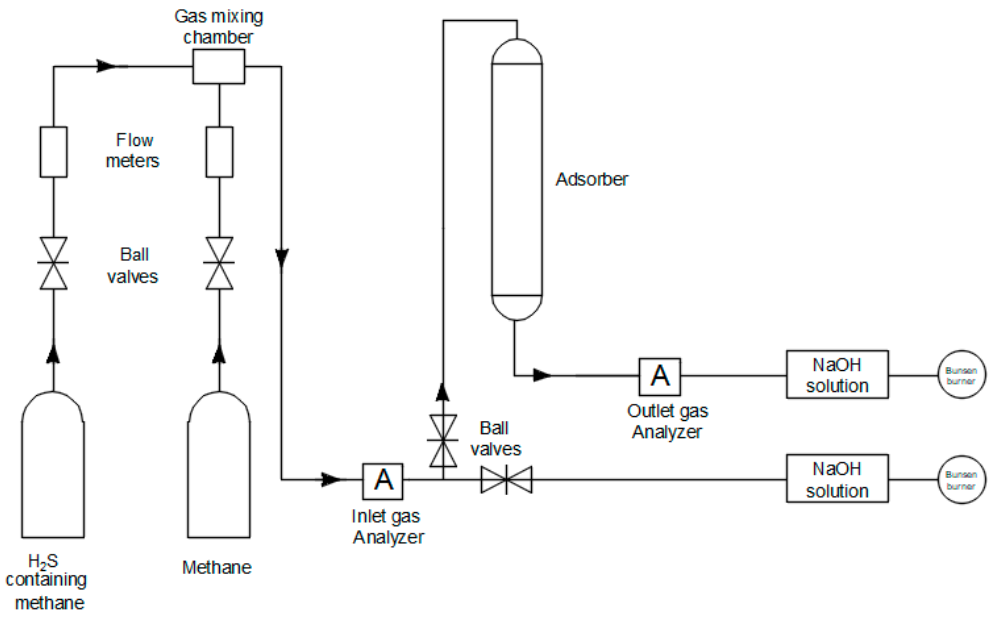

Figure 1. Laboratory set-up for H_2S adsorption.

2.5. Adsorption capacity

Adsorption capacity is defined as the ratio of adsorbed molecular amount to adsorbent mass, and it is typically represented in units of mmol/g or mg/g [14]. The efficiency of the adsorbent is assessed by finding its adsorption capacity. There are two types of adsorption capacity effective and saturated adsorption capacity. The former is calculated when the outlet concentration of H_2S is 1 ppm,

Preprints (www.preprints.org) | NOT PEER-REVIEWED | Posted: 5 December 2023 doi:10.20944/preprints202312.0233.v1

regardless of what the inlet concentration is. However, the latter is calculated when the outlet H_2S concentration reaches the initial concentration. Consequently, the saturated adsorption capacity is always greater than the effective adsorption capacity. Since, in most cases, effective adsorption capacity is important, in this study we were limited to its calculation alone. The following equation was used to calculate effective adsorption capacity.

$$C_{ads} = \frac{Q_{tot} \cdot MW \cdot [C_{in} \cdot t_1 - (t_1 - t_0) \cdot 0.5]}{V_m \cdot m \cdot 10^3} \quad (1)$$

where, Q_{tot}=total gas flow rate (*Nl/h*)
MW=molecular weight of H_2S (g/mol)
C_{in}=inlet H_2S concentration (ppmv)
t_1=breakthrough time when the outlet concentration is 1 ppmv (h)
t_0=breakthrough time at the last detection of 0 ppmv (h)
V_m=molar volume (24,414 Nl/mol)
m=mass of adsorbent material (g).

2.6. Methodology

To evaluate the material's efficacy in removing H_2S, dynamic tests were conducted. 13X spherical pellets with an average particle diameter in the 3–5 mm range and its Ag- ion-exchanged samples were used for the main part of the experiments. Ag The zeolite adsorbents were heated in an oven at 110 *℃* overnight in order to remove any residual gases and traces of humidity that were present inside the pores. After the heating process was complete, the zeolite adsorbents were cooled and stored in a desiccator. The amount of samples was 10.00 g for each test measured after thermal treatment. Adsorption runs were carried out on zeolite samples, obtaining for each set of operating conditions the corresponding breakthrough curve. To produce an adequate concentration of H_2S (i.e., 150ppm, 300 pm, 500ppm), 5000 ppm of H_2S in methane is diluted with methane. Within a certain amount of time, the generated gas was flown to the H_2S scrubber in order to guarantee that the proper concentration of H_2S was reached. Afterwards, a gas mixture containing the desired concentration of H_2S was passed through the adsorber and inlet and outlet H_2S concentrations were measured at every secund to achieve accurate results.

3. Results and discussion

3.1. XRD analysis

The XRD patterns corresponding to 13X and AgI-13X, AgII-13X were presented in Figure 2. The samples feature significant crystallinity, as shown by the strength and broadening of the XRD peaks. The investigated samples showed mainly a crystalline phase composed of sodium aluminum silicate ($Na_{14}Al_{14}Si_{34}O_{96}$) according to the PDF card no. 04-010-5065. The main diffraction peaks at 2 θ = 6.1, 10.0, 11.9, 15.2, 18.3, 20.11 23.2, 26.9, 31.0 are characteristic of the Faujasite structure (JCPDS No: 12-0228) [24]. Between 5° and 15° of 2Theta the characteristic bump was identified characteristic for the amorphous phase. In this part, some of the Ag-based compounds could be identified, however not in the crystalline phase. No significant difference was observed between fresh 13X and the Ag modified samples. It should be noted, however, that the intensity of some peaks for the samples that had been exchanged with silver was diminished. It indicates that the crystal structure of the 13X molecular sieve remains intact after Ag ion-exchange treatment.

Preprints (www.preprints.org) | NOT PEER-REVIEWED | Posted: 5 December 2023 doi:10.20944/preprints202312.0233.v1

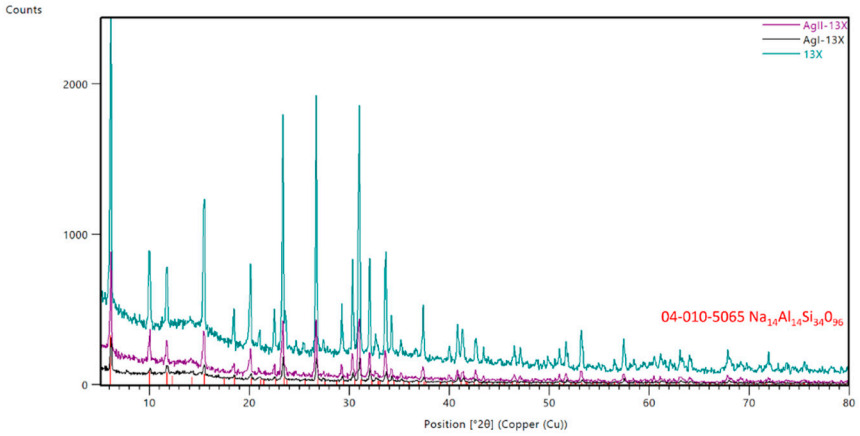

Figure 2. XRD pattern registered for the 13X, AgI-13X and AgII-13X samples.

3.2. SEM images

Figure 3 shows the SEM images of the samples. The framework of the Faujasite zeolite is built by connecting sodalite cages by six rings [25]. SEM analysis verified that both silver modified and fresh 13X are composed of very well- shaped crystallites with a spherical (octahedral) morphology. However, the fresh 13X molecular sieve shows much smoother surfaces as compared to the silver ion-exchanged 13X particles. Moreover, after the ion-exchange process, some of 13X particles cracked, suggesting that lattice destruction might happen during the ion-exchange or high-temperature calcination. These findings are also compatible with the findings of the XRD investigation. Additionally, it is evident that when the ion exchange rate rose in silver modified 13X, the quantity of minor additives in its surface morphology also increased. It is possible to attribute the smaller particles that are found between the zeolite crystals to the binder, which is composed of clay and is utilized in the process of shaping the crystals into beads.

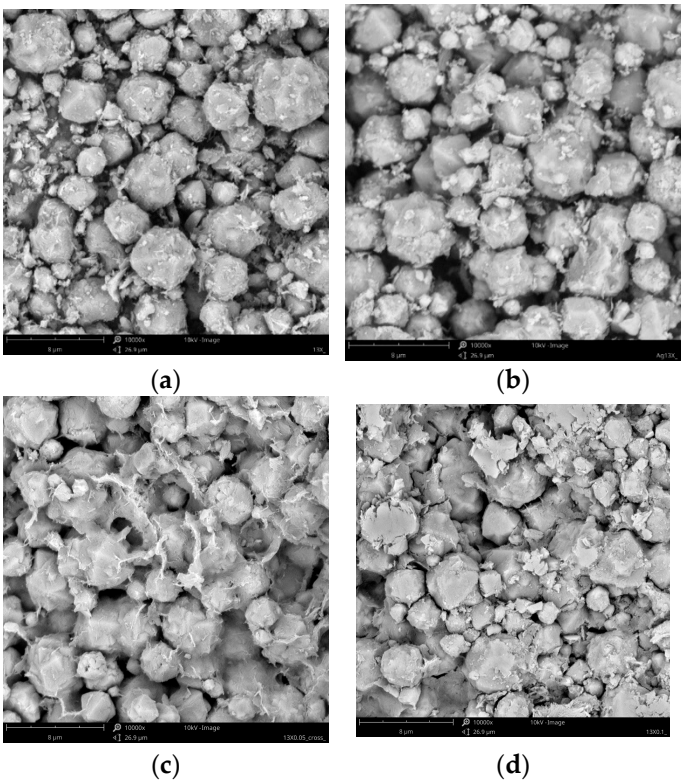

Preprints (www.preprints.org) | NOT PEER-REVIEWED | Posted: 5 December 2023 doi:10.20944/preprints202312.0233.v1

Figure 3. SEM images of (**a**) 13X; (**b**) AgI-13X; (**c**)AgII-13X, and (**d**)AgIII-13X. mag. 10000×.

Compositional characterization of the samples was done by energy dispersive X-ray spectroscopy (EDS) during SEM image acquisition. The element content in the samples was shown in Table 1. It can be seen that the high weight concentration of silver in AgI-13X (10.24 wt. %), AgII-13X (21.38 wt. %) and AgIII-13X (32.38 wt. %) confirmed ion exchange was carried out successfully. Since alkaline metals tend to exchange with silver ions, it can be confirmed that Na^+ cations contained in zeolite are replaced by Ag^+ cations. This can be confirmed by a decrease in Na^+ cations and an increase in Ag^+ cations (Table 1).

Table 1. The element content in 13X, AgI-13X, AgII-13X, and AgIII-13X was determined by the EDS analysis.

Element	Elemental Composition in wt.%			
	13X	**AgI-13X**	**AgII-13X**	**AgIII-13X**
O	55.81	51.83	46.80	39.24
Si	21.20	18.93	16.20	14.31
Al	15.74	12.27	9.40	11.13
Na	6.89	5.79	2.38	2.07
Mg	0.35	0.94	1.55	0.43
Ag	-	10.24	21.32	32.38
Σ	99.99	100	97.65	99.56

3.3. BET analysis analysis

The specific surface area was determined by low temperature nitrogen adsorption (ASAP 2020, Micromeritics Inc., Norcross, GA, USA) using the Brunauer–Emmett–Teller equation [26]. Prior to taking the nitrogen adsorption measurements, each selected sample was outgassed for 24 h at 350℃. The BET surface area of the samples is given in **Table 2**. The BET surface area was calculated 501.33 m^2/g for 13X. However, BET surface area was influenced by the ion-exchange of Ag. An increase in the quantity of silver ions most likely contributed to a decrease in the BET surface area, since the silver ion-exchange of 13X resulted in a marginal decrease in the specific surface area of AgIII-13X from 501.33 to 405 m^2/g. Similar findings were given by Chen et.al.: the BET-specific surface area of silver exchanged X was reduced by 33% [21].

Table 2. BET surface area of the samples.

Adsorbents	BET surface area (m^2/g)
13X	501.33
AgI-13X	436
AgII-13X	416
AgIII-13X	405

3.4. H_2S adsorption

The effects of inlet concentration were measured in samples with H_2S concentration of 150 ppm, 300 ppm and 500 ppm at ambient temperature. The breakthrough curves for 13X and modified zeolites were demonstrated in Figure 4. The concentration of H_2S in the outlet stream is zero for a significant amount of time before it breaks through. The experiments were stopped when the outlet concentration reached 10% of the initial concentration, indicating an effective adsorption time [27]. Adsorption capacity of the 13X, AgI-13X, AgII-13X, and AgIII-13X was calculated from the experimental breakthrough curves and was shown in Table 3. Breakthrough time was determined when the outlet concentration is 1 ppm. Experiments were run until the outlet concentration reached 10% of its initial concentration to show how the breakthrough curve evolved after breakthrough time. Increased inlet H_2S concentration resulted in earlier breakthrough times for all samples, as

Preprints (www.preprints.org) | NOT PEER-REVIEWED | Posted: 5 December 2023 doi:10.20944/preprints202312.0233.v1

anticipated. The 13X molecular sieve exhibited the earliest breakthrough time over all concentration range (150-500). It is noteworthy to mention that the breakthrough time for AgIII-13X was detected earlier than that of AgII-13X. However, the breakthrough curves demonstrated that AgIII-13X is capable of adsorbing substantial quantities of H_2S molecules even after breakthrough time. Across all ranges, the most lates breakthrough time for AgII-13X samples was discovered, indicating their high effective adsorption capacity.

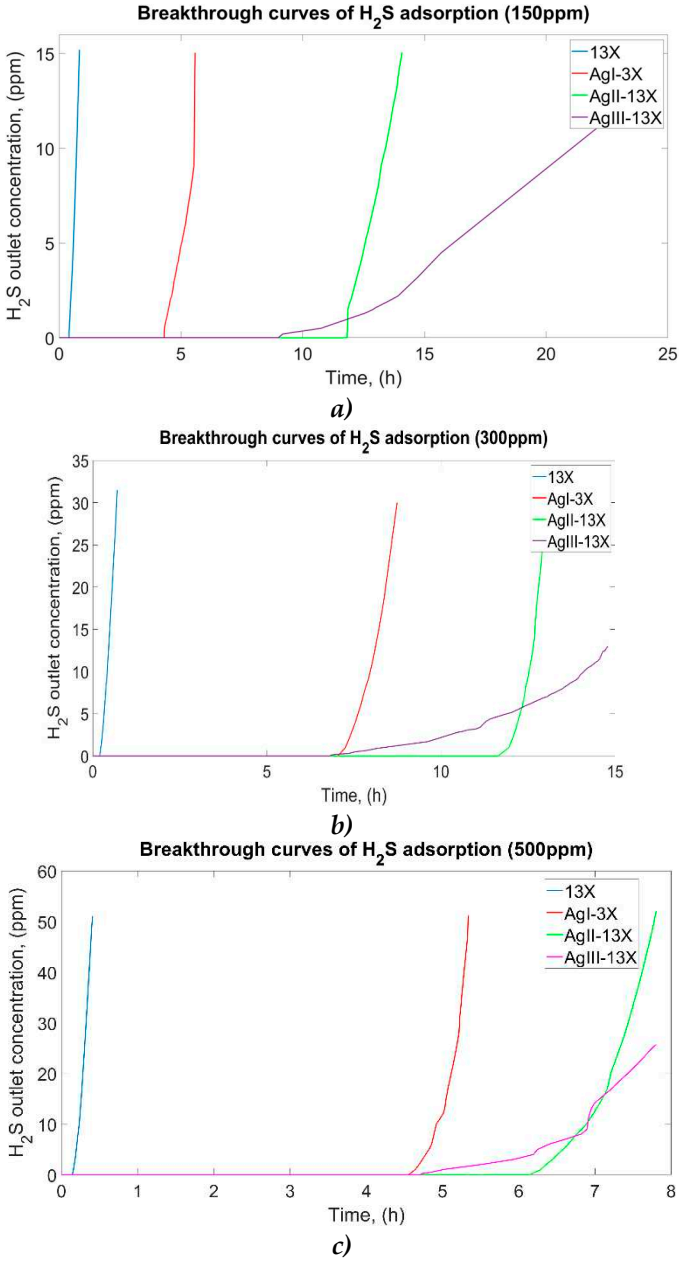

Figure 4. Breakthrough curves of zeolites in the range of 150-500 ppm H_2S in methane.

Table 3. Adsorption capacity of the samples.

Adsorbents	Effective adsorption capacity (mg/g)		
	150 ppm	300 ppm	500 ppm
13X	0.238	0.254	0.26
AgI-13X	2.405	7.92	8.44
AgII-13X	6.47	13.05	11.44
AgIII-13X	4.92	9.1	9.15

Preprints (www.preprints.org) | NOT PEER-REVIEWED | Posted: 5 December 2023 doi:10.20944/preprints202312.0233.v1

3.5. Effect of inlet gas composition

The influence of H_2S concentration in the inlet gas composition was evaluated to determine its impact on adsorption capacity. Initially, three concentrations of H_2S in natural gas, 150 ppm, 300 ppm, and 500 ppm were considered. The breakthrough curve, the corresponding breakthrough time, and the effective H_2S adsorption capacity are shown in Figure 4 and Table 3, respectively. When high H_2S concentrations 500 ppm were used, the breakthrough was reached, as expected, significantly earlier (Figure 4.c) with respect to the concentration of 150 ppm. At a 300 ppm H_2S inlet concentration, a greater adsorption capacity of 13.05 mg/g was achieved for AgII-13X. The lowest adsorption capacity of 0.238 mg/g was observed for non-modified 13X when the H_2S inlet concentration was 150 ppm. Table 4 provides the breakthrough times for the samples.

Table 4. Breakthrough time for the 13X, AgI-13X, AgII-13X, and AgIII-13X in the range of 150-500ppm.

Adsorbents	Breakthrough time (h)		
	150 ppm	**300 ppm**	**500 ppm**
13X	0.435833	0.232778	0.1425
AgI-13X	4.403889	7.253611	4.638611
AgII-13X	11.84806	11.9475	6.284444
AgIII-13X	11.87917	8.338889	5.03

3.6. Effect of Ag concentration

The effect of the concentration of Ag ions on the adsorption capacity of modified zeolite towards H_2S uptake was investigated in the range of molar concentrations of 0.02-0.1M $AgNO_3$ water solution. The results are reported in Figure 4 and Table 3 respectively. It can be seen in Figure 4 that the increase of silver ions on zeolite samples led to an increase in breakthrough time and H_2S adsorption capacity. However, when the silver ion concentration is too large (Figure 4.a for AgIII-13X, 0.1 M $AgNO_3$) the breakthrough time was observed earlier with respect to AgII-13X, resulting in decrease in the adsorption performance. In spite of observing earlier breakthrough time for AgIII-13X, breakthrough curve changed marginally compared to other samples. It is understandable that excessive metal ions might clog zeolites' pores and prevent H_2S from adsorbing on AgIII-13X samples. The use of high $AgNO_3$ solution concentration results in an increase in the cost of the adsorbent. Therefore, modification of the 13X molecular sieve using 0.05 M $AgNO_3$ solution was believed appropriate. It was determined that AgII-13X possessed a greater adsorption capacity, measuring 13.06 mg/g. AgII-13X showed about 50 times more adsorption capacity than non-modified 13X, which only had 0.238 mg/g of adsorption capacity.

3.7. Adsorption mechanism

After the procedure was started, it was observed that the initially white adsorbent surface underwent a color change, transitioning to a darker shade. This alteration in coloration served as an indication that chemical adsorption was taking place. Sodium (Na^+) ions present in 13X replace silver (Ag^+) cations, leading to a subsequent chemical reaction with hydrogen sulfide (H_2S) molecules, resulting in the formation of black silver sulfide (Ag_2S). π-complexation and sulfur-metal (S-M) bond formation may take place between sulfur compounds and metal ions. Previous research also stated that [21] the S-M bond was found to exist between the metal ion and H_2S. The Ag-sulfide bond was found to have the highest strength according to the Mayer bond order (0.639), which was determined by employing Density Functional Theory (DFT).

3.8. Adsorption isotherms

The Langmuir and Freundlich adsorption models were applied to assess adsorption parameters and to investigate adsorption mechanisms at ambient temperature. The Langmuir model describes monolayer adsorption of adsorbate onto homogenous solid surface sites, while the Freundlich model

Preprints (www.preprints.org) | NOT PEER-REVIEWED | Posted: 5 December 2023 doi:10.20944/preprints202312.0233.v1

does not have a maximum adsorption limit. Two adsorption models were implemented for AgII-13X since it showed high adsorption capacity (Figure 5).

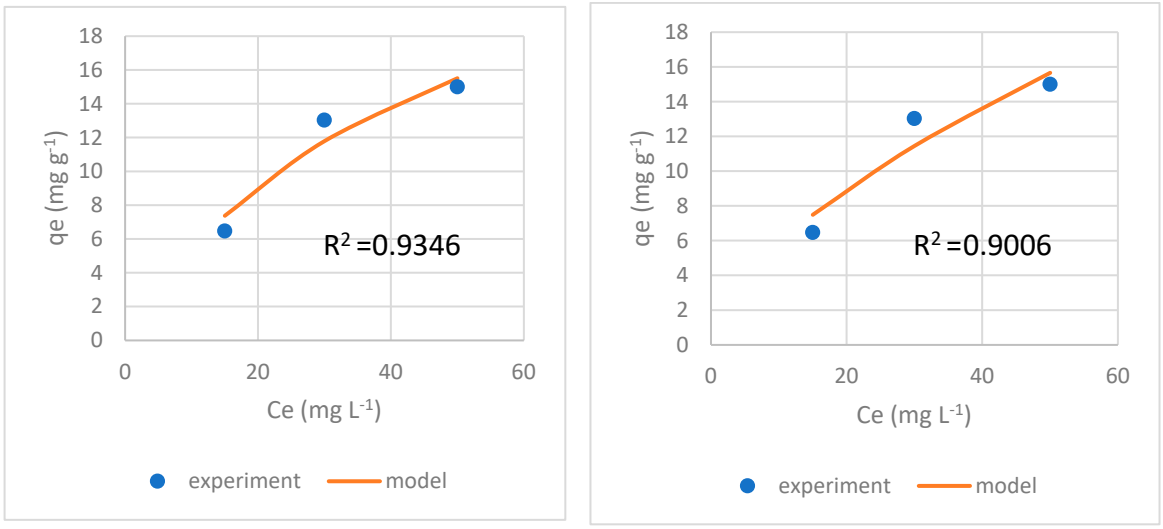

a) b)

Figure 5. Langmuir a) and Freundlich b) adsorption isotherm models at ambient temperature for AgII-13X.

Following Langmuir isotherm equation was used:

$$q_e = \frac{K_L q_{max} C_e}{1 + C_e K_L} \quad (2)$$

where, q_e and C_e are the H_2S uptake and equilibrium concentration, respectively, K_L is the Langmuir isotherm constant related to the binding energy, and q_{max} is the theoretically calculated adsorption capacity.

The Freundlich model adsorption parameters were obtained using following equation (4):

$$q_e = K_F * C_e^{1/n} \quad (3)$$

where, K_F is a Freundlich constant or maximum adsorption capacity, C_e is the concentration of adsorbate under equilibrium condition (mg/L), q_e is the amount of adsorbate adsorbed per unit mass of adsorbent (mg/g), is the value indicating the degree of linearity between the adsorbate solution and the adsorption process.

Table 4. Adsorption isotherm parameters for AgII-13X.

Langmuir	Value	Freundlich	Value
K_L (μM-1)	0.002229	***K_F (mmol m-2 μM-1/n)***	***0.347795***
R^2 (Ce vs qe)	0.9346	***R_2 (Ce vs qe)***	0.9006
q_{max} (mg g-1)	29.42685	***n***	1.632228

The average determination coefficient (R^2) for AgII-13X zeolites was 0.9346 in Langmuir and 0.9006 in Freundlich, indicating that Langmuir's isothermal model is better in our case. The maximum adsorption capacity was calculated 29.42 mg/g that is higher then effective adsorption capacity of 13.06 mg/g.

4. Conclusions

Several promising results have been reported on the modification of the commercially available 13X molecular sieve adsorbent with silver ions and its application in the separation of H_2S from various mixtures. However, there is no comprehensive study in the available literature on the extraction of H_2S from natural gas using Ag-modified adsorbents. In this work, 13X molecular sieve

Preprints (www.preprints.org) | NOT PEER-REVIEWED | Posted: 5 December 2023 doi:10.20944/preprints202312.0233.v1

was modified with different concentrations of $AgNO_3$ solution and it was used to purify natural gas from H_2S.

The results showed that the ion exchange of 13X molecular sieve with silver ions has a positive effect on the increase in adsorbent capacity. The highest adsorption capacity of 13.05 mg/g was reached using AgII-13X zeolite and is highly effective at removing H_2S from a variety of gases that contain methane.

Author Contributions: Conceptualization, M.A., M.H.A.-R. and J.W.; Supervision, M.H.A.-R. and J.W.; Visualization, M.A., M.H.A.-R. and J.W.; Writing—original draft, M.A.; Writing—reviewing and editing M.H.A.-R. and J.W.

Funding: This research received no external funding.

Conflicts of Interest: The authors declare no conflict of interest.

References

1. *International Energy Agency (2023), World Energy Outlook 2023, IEA, . Licence: Creative Commons Attribution CC BY-NC-SA 4.0.*
2. Sebastien Duval, "Natural gas sweetening," in *Surface Process, Transportation, and Storage*, 2023, pp. 37–78. doi: 10.1016/b978-0-12-823891-2.00013-2.
3. S. Mokhatab, W. A. Poe, and J. Y. Mak, *Handbook of natural gas transmission and processing: Principles and practices*. 2018. doi: 10.1016/C2017-0-03889-2.
4. M. Hedayat, M. Soltanieh, and S. A. Mousavi, "Simultaneous separation of H_2S and CO_2 from natural gas by hollow fiber membrane contactor using mixture of alkanolamines," *J. Memb. Sci.*, vol. 377, no. 1–2, pp. 191–197, 2011, doi: 10.1016/j.memsci.2011.04.051.
5. M. S. Shah, M. Tsapatsis, and J. I. Siepmann, "Hydrogen Sulfide Capture: From Absorption in Polar Liquids to Oxide, Zeolite, and Metal-Organic Framework Adsorbents and Membranes," *Chem. Rev.*, vol. 117, no. 14, pp. 9755–9803, Jul. 2017, doi: 10.1021/acs.chemrev.7b00095.
6. L. H. de Oliveira, J. G. Meneguin, M. V. Pereira, J. F. do Nascimento, and P. A. Arroyo, "Adsorption of hydrogen sulfide, carbon dioxide, methane, and their mixtures on activated carbon," *Chem. Eng. Commun.*, vol. 206, no. 11, pp. 1544–1564, 2019, doi: 10.1080/00986445.2019.1601627.
7. M. C. Castrillon *et al.*, "CO_2 and H_2S Removal from CH_4-Rich Streams by Adsorption on Activated Carbons Modified with K_2CO_3, NaOH, or Fe_2O_3," *Energy and Fuels*, vol. 30, no. 11, pp. 9596–9604, 2016, doi: 10.1021/acs.energyfuels.6b01667.
8. N. N. Zulkefli, M. S. Masdar, W. N. Roslam Wan Isahak, J. M. Jahim, S. A. Md Rejab, and C. C. Lye, "Removal of hydrogen sulfide from a biogas mimic by using impregnated activated carbon adsorbent," *PLoS ONE*, vol. 14, no. 2. 2019. doi: 10.1371/journal.pone.0211713.
9. Y. Belmabkhout *et al.*, "Natural gas upgrading using a fluorinated MOF with tuned H_2S and CO_2 adsorption selectivity," *Ind. Eng. Chem. Res.*, vol. 25, no. 16, p. 111886, Jul. 2020, doi: 10.1021/la903238y.
10. G. Liu *et al.*, "Enabling Fluorinated MOF-Based Membranes for Simultaneous Removal of H_2S and CO_2 from Natural Gas," *Angew. Chemie - Int. Ed.*, vol. 57, no. 45, pp. 14811–14816, 2018, doi: 10.1002/anie.201808991.
11. A. Mohammadi, Z. Saadati, and S. Joohari, "Comparison of the adsorption of H_2S by ZnO–TiO_2 and Ni–ZnO–TiO_2 nanoparticles: An adsorption isotherm and thermodynamic study," *Environ. Prog. Sustain. Energy*, vol. 38, no. 6, 2019, doi: 10.1002/ep.13258.
12. D. Jiang *et al.*, "Cu-Zn-Al mixed metal oxides derived from hydroxycarbonate precursors for H_2S removal at low temperature," *Appl. Surf. Sci.*, vol. 256, no. 10, pp. 3216–3223, 2010, doi: 10.1016/j.apsusc.2009.12.008.
13. T. Yu, Z. Chen, Z. Liu, J. Xu, and Y. Wang, "Review of Hydrogen Sulfide Removal from Various Industrial Gases by Zeolites," *Separations*, vol. 9, no. 9, 2022, doi: 10.3390/separations9090229.
14. M. Abdirakhimov, M. H. Al-Rashed, and J. Wójcik, "Recent Attempts on the Removal of H_2S from Various Gas Mixtures Using Zeolites and Waste-Based Adsorbents," *Energies*, vol. 15, no. 15, p. 5391, Jul. 2022, doi: 10.3390/en15155391.
15. Y. Huang, W. Su, R. Wang, and T. Zhao, "Removal of typical industrial gaseous pollutants: From carbon, zeolite, and metal-organic frameworks to molecularly imprinted adsorbents," *Aerosol Air Qual. Res.*, vol. 19, no. 9, pp. 2130–2150, 2019, doi: 10.4209/aaqr.2019.04.0215.

Preprints (www.preprints.org) | NOT PEER-REVIEWED | Posted: 5 December 2023 doi:10.20944/preprints202312.0233.v1

16. L. Sigot, M. Fontseré Obis, H. Benbelkacem, P. Germain, and G. Ducom, "Comparing the performance of a 13X zeolite and an impregnated activated carbon for H_2S removal from biogas to fuel an SOFC: Influence of water," *Int. J. Hydrogen Energy*, vol. 41, no. 41, pp. 18533–18541, 2016, doi: 10.1016/j.ijhydene.2016.08.100.
17. F. Bandarchian and M. Anbia, "Conventional hydrothermal synthesis of nanoporous molecular sieve 13X for selective adsorption of trace amount of hydrogen sulfide from mixture with propane," *J. Nat. Gas Sci. Eng.*, vol. 26, pp. 1380–1387, 2015, doi: 10.1016/j.jngse.2015.08.019.
18. K. Yang, B. Su, L. Shi, H. Wang, and Q. Cui, "Adsorption Mechanism and Regeneration Performance of 13X for H_2S and SO_2," *Energy & Fuels*, vol. 32, no. 12, pp. 12742–12749, Dec. 2018, doi: 10.1021/acs.energyfuels.8b02978.
19. A. Starke, C. Pasel, C. Bläker, T. Eckardt, J. Zimmermann, and D. Bathen, "Investigation of the Adsorption of Hydrogen Sulfide on Faujasite Zeolites Focusing on the Influence of Cations," *ACS Omega*, vol. 7, no. 48, pp. 43665–43677, 2022, doi: 10.1021/acsomega.2c04606.
20. L. Barelli, G. Bidini, L. Micoli, E. Sisani, and M. Turco, "13X Ex-Cu zeolite performance characterization towards H_2S removal for biogas use in molten carbonate fuel cells," *Energy*, vol. 160, pp. 44–53, 2018, doi: 10.1016/j.energy.2018.05.057.
21. X. Chen, B. Shen, H. Sun, and G. zhan, "Ion-exchange modified zeolites X for selective adsorption desulfurization from Claus tail gas: Experimental and computational investigations," *Microporous Mesoporous Mater.*, vol. 261, no. November 2017, pp. 227–236, 2018, doi: 10.1016/j.micromeso.2017.11.014.
22. P. Kumar *et al.*, "H_2S adsorption by Ag and Cu ion exchanged faujasites," *Microporous Mesoporous Mater.*, vol. 146, no. 1–3, pp. 127–133, 2011, doi: 10.1016/j.micromeso.2011.05.014.
23. S. Kulawong, R. Artkla, P. Sriprapakhan, and P. Maneechot, "Biogas purification by adsorption of hydrogen sulphide on NaX and Ag-exchanged NaX zeolites," *Biomass and Bioenergy*, vol. 159, no. November 2021, p. 106417, 2022, doi: 10.1016/j.biombioe.2022.106417.
24. S. A. Bradley, R. W. Broach, T. M. Mezza, S. Prabhakar, and W. Sinkler, *Zeolite Characterization*. 2010. doi: 10.1002/9783527629565.ch4.
25. C. Baerlocher and L.B.McCusker, "Database of Zeolite Structures, http://www.iza-structure.org/databases/," *Database of Zeolite Structures*. [Online]. Available: http://www.iza-structure.org/databases/
26. S. Brunauer, P. H. Emmett, and E. Teller, "Adsorption of Gases in Multimolecular Layers," *J. Am. Chem. Soc.*, vol. 60, no. 2, pp. 309–319, 1938, doi: 10.1021/ja01269a023.
27. L. Zhu *et al.*, "Modification of zeolite by metal and adsorption desulfurization of organic sulfide in natural gas," *J. Nat. Gas Sci. Eng.*, vol. 69, no. February, p. 102941, 2019, doi: 10.1016/j.jngse.2019.102941.

Disclaimer/Publisher's Note: The statements, opinions and data contained in all publications are solely those of the individual author(s) and contributor(s) and not of MDPI and/or the editor(s). MDPI and/or the editor(s) disclaim responsibility for any injury to people or property resulting from any ideas, methods, instructions or products referred to in the content.